microbial biotechnology

Additive effects of metal excess and superoxide, a highly toxic mixture in bacteria

Anne Soisig Steunou,* Marion Babot, Marie-Line Bourbon, Reem Tambosi, Anne Durand, Sylviane Liotenberg, Anja Krieger-Liszkay, Yoshiharu Yamaichi and Soufian Ouchane** (iD)
Institute for Integrative Biology of the Cell (I2BC), CEA, CNRS, Université Paris-Saclay, 91198, Gif-sur-Yvette, France.

Summary

Heavy metal contamination is a serious environmental problem. Understanding the toxicity mechanisms may allow to lower concentration of metals in the metal-based antimicrobial treatments of crops, and reduce metal content in soil and groundwater. Here, we investigate the interplay between metal efflux systems and the superoxide dismutase (SOD) in the purple bacterium *Rubrivivax gelatinosus* and other bacteria through analysis of the impact of metal accumulation. Exposure of the Cd^{2+}-efflux mutant $\Delta cadA$ to Cd^{2+} caused an increase in the amount and activity of the cytosolic Fe-Sod SodB, thereby suggesting a role of SodB in the protection against Cd^{2+}. In support of this conclusion, inactivation of *sodB* gene in the $\Delta cadA$ cells alleviated detoxification of superoxide and enhanced Cd^{2+} toxicity. Similar findings were described in the Cu^+-efflux mutant with Cu^+. Induction of the Mn-Sod or Fe-Sod in response to metals in other bacteria, including *Escherichia coli*, *Pseudomonas aeruginosa*, *Pseudomonas putida*, *Vibrio cholera* and *Bacillus subtilis*, was also shown. Both excess Cd^{2+} or Cu^+ and superoxide can damage [4Fe-4S] clusters. The additive effect of metal and superoxide on the [4Fe-4S] could therefore explain the hypersensitive phenotype in mutants lacking SOD and the efflux ATPase. These findings underscore that ROS defence system becomes decisive for bacterial survival under metal excess.

Introduction

Heavy metal pollution, mainly caused by anthropogenic activities, may have adverse effects on the ecosystems and living organisms unless sustainable management practices are implemented. Cu^{2+} and Cd^{2+} pollution originating from activities including excessive use of fertilizers, antimicrobials and agrochemicals is an important environmental concern (Ballabio *et al.*, 2018).

https://ec.europa.eu/environment/integration/research/newsalert/pdf/agricultural_management_practices_influence_copper_concentrations_european_topsoils_518_na2_en.pdf

Metal pollution contributes also to the selection and spread of antibiotic resistance factors. In fact, cross-resistance in bacteria can occur through transfer of genes encoding efflux pumps that can expel antibiotics in addition to metals (Baker-Austin *et al.*, 2006; Rensing *et al.*, 2018; Asante and Osei Sekyere, 2019). Metal pollution affects groundwater and soils properties by altering the microbial diversity and evenness (Nunes *et al.*, 2016). Limiting the concentration of heavy metals in agrochemicals or in metal-based antimicrobial treatments can lead to a sustainable use of metals in agriculture and farming (Turner, 2017) and may limit the metal-related co-selection for metal and antibiotic resistance in bacteria.

In contaminated soils, exposed organisms have to deal with excess metal. In bacteria, most metal ions presumably reach the bacterial cytoplasm through porins and specific or non-specific transporters in the inner membrane. The lack of rigorous control or specific uptake system for some metals is often compensated for by the presence of effective efflux systems. This allows cells to tolerate the excess of metal(s) in their immediate environment by expelling the surplus of metal ions (Arguello *et al.*, 2007; von Rozycki and Nies, 2009; Capdevila *et al.*, 2017; Chandrangsu *et al.*, 2017). The P_{1B}-type ATPases family of heavy metal transporters is the most frequently present in bacteria. They are efficient efflux pumps that extrude excess of toxic metal ions such as copper (Cu^+), zinc (Zn^{2+}), cadmium (Cd^{2+}) or silver (Ag^+) from the cytoplasm to the

periplasm in which metal is handled by other detoxifying proteins (Arguello *et al.*, 2007). The effectiveness of these metal efflux systems prevents the molecular and physiological damages that metal can cause. Therefore, mutants defective in metal homoeostasis machineries, specifically in the efflux systems, shed light on the toxicity mechanisms and the molecular events following metal accumulation within the cell. Lines of evidence showed that while excess of metal can cause damage to [4Fe-4S] clusters and mismetallation of metalloproteins under strict anaerobic condition (Macomber and Imlay, 2009), contribution of reactive oxygen species (ROS) should be taken into account under aerobic condition.

Superoxide is produced in presence of oxygen by some aerobic respiratory complexes and other non-respiratory flavoproteins, like the lipoamide or xanthine dehydrogenases. It can directly damage exposed catalytic [4Fe-4S] clusters in dehydratases or mononuclear Fe^{2+} enzymes, or indirectly damage other cell components by contributing to the production of hydroxyl radicals (Imlay, 2013; Imlay, 2019). To deal with superoxide in the cytoplasm, bacteria possess either one or two superoxide dismutases (Fe-Sod and Mn-Sod) whose expression is differently regulated by redox-cycling compounds and by iron (Imlay, 2013; Imlay, 2019). In enteric bacteria such as *Escherichia (E.) coli*, *sodA* gene is regulated by the SoxRS system. The transcriptional factor SoxR functions as a sensor of oxidative stress in response to changes in the redox state of its [2Fe-2S] cluster (Imlay, 2013; Kobayashi, 2017; Imlay, 2019). SoxR activates the transcriptional factor SoxS that in turn induces the transcription of many genes including *sodA*. Nonetheless, the majority of SoxR regulons in bacteria, including *Vibrio* and *Pseudomonas*, lack the *soxS* gene (Dietrich *et al.*, 2008). Expression of Sod in these bacteria does not involve SoxR and relies mainly on iron homoeostasis and regulators. In *E. coli* and other bacteria, when iron is available, the Fe^{2+}-Fur repressor inhibits Mn-Sod and small RNA RyhB production and activates the Fe-Sod synthesis. In contrast, under iron limitation, Fur is inactivated, which induces the synthesis of the Mn-Sod and the transcription of the small RyhB RNA. RyhB interaction with Fe-Sod mRNA triggers degradation of the mRNA and thus promotes decrease of Fe-Sod in the cells (Masse and Gottesman, 2002; Imlay, 2013; Imlay, 2019).

Metal stress promotes increase in the level of oxidative stress-associated defence enzymes such as superoxide dismutases (SOD), catalases and peroxidases, which suggest elevated ROS in metal-stressed cells (Krumschnabel *et al.*, 2005; Macomber *et al.*, 2007; Helbig *et al.*, 2008; Ray *et al.*, 2013; Xu *et al.*, 2019). The involvement of these enzymes in metal stress

response was further supported by the metal-sensitive phenotype of *E. coli* mutant of which two genes encoding SOD were concomitantly inactivated (Geslin *et al.*, 2001).

Macomber and co-workers reported that while copper did not induce significant oxidative DNA damage in copper-overloaded *E. coli* cells, they exhibited increased catalase (KatG and KatE) and superoxide dismutase activities. This suggested an induction of SoxRS regulons and the presence of elevated amounts of hydrogen peroxide and superoxide in these cells (Macomber *et al.*, 2007). Metals such as Fe^{2+} and Cu^+ are redox-active ions which, in presence of oxygen, can induce the formation of reactive oxygen species *via* Fenton and Haber–Weiss-type reactions (Gunther *et al.*, 1995). These metals are also toxic under anaerobic condition, as Cu^+ was shown to directly poison bacteria by damaging the exposed [4Fe-4S] clusters of dehydratases in *E. coli* (Macomber and Imlay, 2009) and those of porphyrin biosynthesis enzymes in the photosynthetic bacterium *Rubrivivax (R.) gelatinosus* and the human pathogen *Neisseria gonorrhea* (Azzouzi *et al.*, 2013; Djoko and McEwan, 2013). Toxicity of non-redox-active metals such as Cd^{2+} or Zn^{2+} was also associated with destruction of exposed [4Fe-4S] clusters, and release of iron, which in turn might produce hydroxyl radicals via the Fenton reaction (18).

In the present study, we investigated the role of superoxide dismutase and superoxide stress in heavy metal toxicity. We found that Cd^{2+} or Cu^+ stress induced the expression and activity of the cytosolic Fe-Sod or Mn-Sod in many bacteria including *R. gelatinosus*, *E. coli*, *Vibrio (V.) cholerae*, *Pseudomonas (P.) aeruginosa*, *P. putida* and *Bacillus (B.) subtilis*, when the metal efflux systems are missing.

Although SOD induction by excess metal was previously reported in many transcriptomic data sets, the importance and consequences of SOD inactivation under excess metal in metal efflux deficient mutants were never reported. Here, the Cd^{2+} and Cu^+ hypersensitive phenotypes of mutants lacking SOD along with the Cd^{2+} and Cu^+-ATPases, respectively, were shown to emphasize the importance of SOD and ROS detoxification in metal toxicity. Altogether, the data demonstrated the involvement of SOD in the protection of heavy metal-exposed cells and shed light on the synergy of excess metal and superoxide in heavy metal toxicity.

Results

Induction of a 22 kDa protein in cadR⁻ and ΔcadA deficient strains

To deal with toxic Cd^{2+} exposure, bacteria usually induce the expression of gene encoding the metal efflux

ATPase, CadA (also known as ZntA in some species, as it expels Zn^{2+} as well). The major transcriptional regulator CadR interacts with Cd^{2+}, thereby allowing induction of the expression of the CadA ATPase. While these genes are widely distributed in bacterial species, purple photosynthetic bacteria can encounter Cd^{2+} in their environment and are therefore suitable models to assess the effect of Cd^{2+} on their growth. Requirement for CadR in CadA expression and metal tolerance was assessed in the purple photosynthetic bacterium *R. gelatinosus* wild-type and *cadR⁻* mutant cells. To this end, total cell extracts from overnight culture of wild-type and *cadR⁻* mutant grown under photosynthetic condition with different concentrations of $CdCl_2$ were analysed by Western blot. Note that CadA and the periplasmic copper protein CopI can be readily detected by conventional HisProbe due to the presence of histidine-rich motifs within these proteins. In the wild-type, Cd^{2+} induced a steady increase in the amount of CadA and CopI proteins (Fig. 1A). In the *cadR⁻* mutant, CadA was not induced below 600 μM of $CdCl_2$. Unexpectedly, however, apparent induction of CadA was observed with excess $CdCl_2$ (800 and 1000 μM). Furthermore, a 22 kDa protein band revealed by the HisProbe was clearly induced up to 600 but not with 800 and 1000 μM of $CdCl_2$ (Fig. 1A). Interestingly, the corresponding band was only slightly expressed in the wild-type cells, even for those challenged with excess Cd^{2+}. Concomitantly to CadA induction, the 22 kDa protein amount decreased upon elevated Cd^{2+} stress (800 and 1000 μM) in the *cadR⁻* mutant (Fig. 1A). Taken together, these data confirmed that Cd^{2+} induced the expression of the Cd^{2+}-efflux ATPase CadA and the production of a 22 kDa protein in CadR-deficient cells. Moreover, these data

suggested a direct link between the expressions of these two proteins. To test this possibility, CadA-deficient mutant Δ*cadA* of *R. gelatinosus* was subjected to Cd^{2+} stress. In contrast to *cadR⁻*, growth of the Δ*cadA* mutant was inhibited beyond 200 μM $CdCl_2$ (see below); therefore, the analysis included only low $CdCl_2$ concentrations. As expected, Cd^{2+} excess (100 or 200 μM) caused an increase in the amount of CadA and CopI proteins, but the amount of the 22 kDa protein remained unchanged in the wild-type strain (Fig. 1B). In contrast, both CopI and the 22 kDa protein were induced in the Cd^{2+}-stressed Δ*cadA* mutant cells (Fig. 1B). Therefore, in the absence of the CadA ATPase, Cd^{2+} induced the expression of the 22 kDa protein which could be involved in Cd^{2+} response and tolerance. Similar results showing the induction of the 22 kDa protein in *cadR⁻* and Δ*cadA* strains were obtained under respiratory (aerobic) condition (Fig. S1). Alongside this study, biochemical experiments in our group suggested that the 22 kDa protein may correspond to the Fe-Sod superoxide dismutase, SodB (unpublished data).

Induction of SodB in response to excess Cd^{2+} in the Δ**cadA** mutant

Various SOD genes encode the enzymes responsible for superoxide dismutation and contribute to the protection of bacteria against ROS (Beyer *et al.*, 1991; Imlay, 2003). These SODs vary by their metal cofactors but also by their subcellular localization. Analysis of the genome of *R. gelatinosus* highlighted the presence of two SOD encoding genes: *sodC* and *sodB*, which, respectively, encode the 15 kDa periplasmic Cu-Zn SodC and a cytosolic 21.5 kDa Fe-Sod. SodB displays
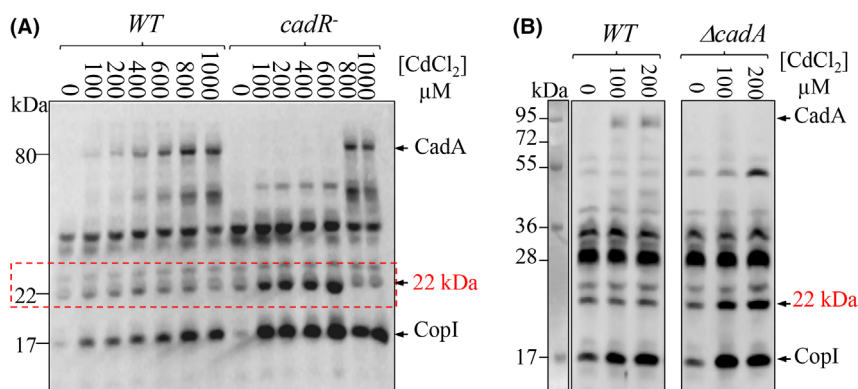

Fig. 1. Induction of His-rich 22 kDa protein in Cd^{2+} efflux pump mutants in *R. gelatinosus*. Induction of CadA, CopI and the 22 kDa proteins in *R. gelatinosus* wild-type (WT) strain, *cadR⁻* (A) and Δ*cadA* mutants (B). Total protein extracts from the same amount of cells (0.1 OD_{680nm}) grown overnight in photosynthetic condition with indicated concentration of $CdCl_2$ were separated on 15% SDS-PAGE and analysed by Western blot using the HRP-HisProbe. Growth of *cadR⁻* with 800 and 1000 μM of $CdCl_2$ started after 3 days (very likely suppressors). CadA, CopI and the 22 kDa protein are indicated.

a five-histidine-rich motif in its amino terminus sequence, suggesting that the HisProbe could allow SodB detection. To demonstrate that SodB corresponded to the 22 kDa band, we disrupted the *sodB* gene by insertion of a kanamycin resistance cassette within the coding region and checked for the presence of the 22 kDa protein. Western blot analysis confirmed that the band at 22 kDa was indeed absent in the inactivated strain Δ*sodB* (Fig. 2A). Next, we tested SOD activity in *R. gelatinosus* Δ*sodB* mutant. It is established that SOD mutants are more sensitive to the redox-cycling agent menadione in the presence of oxygen. The susceptibility of Δ*sodB* to menadione was tested in comparison with the wild-type by disc diffusion assays under photosynthetic and respiratory conditions. The Δ*sodB* mutant was found to be more sensitive to menadione than the wild-type under both conditions. Growth inhibition zone for Δ*sodB* mutant reached 26 and 29 mm, whereas the inhibition diameter only spanned 16 and 18 mm under photosynthetic and aerobic conditions, respectively, for the wild-type strain (Fig. 2B). Complementation of the Δ*sodB* mutant with the *sodB* gene cloned on a replicative plasmid restored a wild-type phenotype on menadione, further confirming the role and activity of SodB in *R. gelatinosus* (Fig. S2). *In-gel* SOD activity assay showed only one active band in the wild-type soluble fraction, which was absent in the Δ*sodB* strain (Fig. 2C). These results strongly indicated that the 22 kDa protein corresponds

to the SodB protein which has bona fide SOD activity. Note that, among *Rubrivivax* strains, two other strains (*R. gelatinosus IL144* and *R. benzoalyticus*) have their *sodB* gene fused with the upstream gene, *xseA*, which encodes the 55-kDa exonuclease VII large subunit (Fig. S3). While RT-PCR experiment showed that these two genes were cotranscribed (Fig. S3), we did not detect any corresponding band at 70 kDa with the HisProbe in all tested conditions (Fig. 1 and Fig. S1). The presence of an internal promoter, a post-transcriptional or post-translational regulatory mechanism may lead to the expression of the intact SodB protein of 22 kDa. Nonetheless, the Δ*xseA* mutant was not sensitive to ROS compared to Δ*sodB* (data not shown). Furthermore, complementation of Δ*sodB* strain with pB*xseAsodB* or pB*sodB* restored a wild-type phenotype (Fig. S2), confirming that XseA did not play a role in the SOD activity.

To further examine the impact of increasing concentration of Cd^{2+} on the SodB expression and activity in the Δ*cadA* mutant under different oxygen tensions, cells were grown under photosynthetic or respiratory condition, and their soluble fractions analysed. Western blot analysis and *in-gel* activity assay showed that the amount and activity of SodB increased in Δ*cadA* cells with increasing cadmium concentration under both growth conditions (Fig. 2D and E). However, the increase in expression and activity was more substantial under respiratory condition (Fig. 2E).
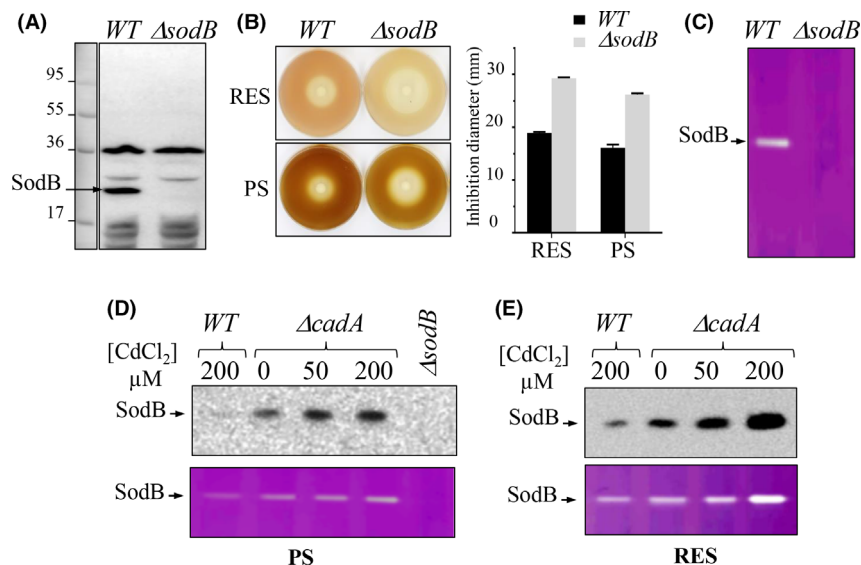

Fig. 2. *R. gelatinosus* SodB expression and activity. (A) Western blot analysis of wild-type (*WT*) and Δ*sodB* mutant cells. Cells were grown by photosynthesis and total protein extracts from the same amount of cells (0.1 OD$_{680nm}$) were analysed by Western blot. (B) Involvement of SodB in oxidative stress under photosynthetic (PS) or respiratory (RES) condition. Representative growth inhibition (left) and mean ± stdev from 3 independent experiments of the diameter of inhibition zone (right) are presented. (C) SOD *in-gel* activity assay of indicated strains. Expression and activity profile of SodB in the *WT*, Δ*cadA* strain after various CdCl$_2$ treatment of cells grown under PS (D) and RES (E) conditions.

Loss of SodB did not influence Cd^{2+} tolerance in the wild-type background, but remarkably, SodB was required in cells unable to detoxify Cd^{2+}

Changes in the amount and activity of oxidative stress-associated defence enzymes including SODs can be used as evidence for an increased oxidative stress in the cell. Yet, direct involvement of SodB in Cd^{2+} tolerance has not been demonstrated. To address this, growth inhibition in presence of increasing concentration of Cd^{2+} was monitored for the wild-type, ΔsodB and ΔcadA strains under respiratory and photosynthetic conditions. ΔsodB and wild-type strains exhibited comparable growth inhibition profiles under both conditions (Fig. 3A and B). In contrast, growth of the ΔcadA mutant was compromised by low concentration of Cd^{2+} (Fig. 3A and B).

The Cd^{2+}-efflux ATPase CadA extrudes Cd^{2+} from the cytoplasm in *R. gelatinosus*. Thus, inactivation of *cadA* led to a decreased Cd^{2+} resistance (Steunou *et al.*, 2020a). Notably, growth inhibition experiments showed that the ΔcadA mutant was more sensitive to cadmium under the respiratory condition than the photosynthetic condition (Fig. 3A and B), which correlated well with the stronger induction of SodB under respiratory condition than photosynthetic condition (Fig. 2D and E). Taken together, these data suggested that SodB would be involved in Cd^{2+} tolerance. Wild-type *R. gelatinosus* was fairly resistant to low concentrations of CdCl$_2$ in both respiratory and photosynthesis conditions (Fig 3A and B). Consistent to no apparent induction of SodB in the wild-type (Fig. 1), ΔsodB mutant exhibited comparable growth inhibition profiles under both conditions (Fig. 3A and B). In contrast, growth of ΔcadAsodB double mutant was dramatically affected by cadmium in both respiratory and photosynthetic conditions in comparison with the wild-type, ΔcadA and ΔsodB strains. Hypersensitivity of ΔcadAsodB strain to the concomitant presence of Cd^{2+} and superoxide was further investigated by disc diffusion assay (Fig. 3C and Fig. S4). To this end, cells were spread on agar plates with or without 25 μM CdCl$_2$. Menadione soaked filter discs were used to assess growth inhibition. Under respiratory condition, growth inhibition zones were comparable, regardless of the supplement of 25 μM CdCl$_2$ for the wild-type, ΔsodB and ΔcadA strains. In contrast, the ΔcadAsodB strain exhibited a very strong phenotype in presence of both CdCl$_2$ and menadione, as growth was completely inhibited on plate (Fig. 3C and Fig. S4). In presence of menadione alone, however, the diameter of bacterium-free zone for ΔcadAsodB and ΔsodB was comparable. Altogether, these data showed that the high toxicity of Cd^{2+} in the absence of the CadA efflux pump was exacerbated by the absence of the superoxide detoxification system.
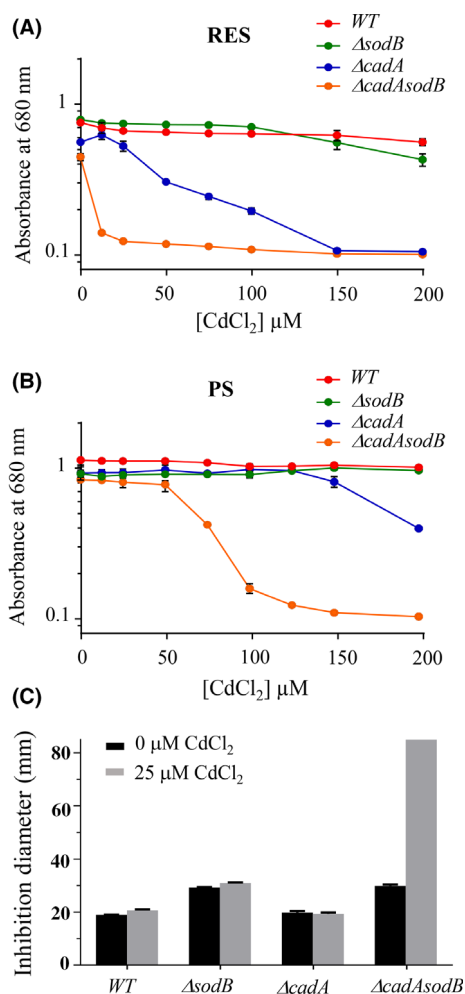

Fig. 3. Involvement of SodB in Cd^{2+} stress in *R. gelatinosus*. Dose–response curves of the wild-type (*WT*), ΔsodB, ΔcadA and ΔcadAsodB strains. Cells were grown for 24 h in the presence of different concentrations of CdCl$_2$ either aerobically (A) or by photosynthesis (B). Results represent the mean of 3 independent experiments. Menadione disc diffusion assay of cells in RES condition with or without 25 μM CdCl$_2$ (C). Results represent mean ± stdev from 3 independent experiments.

SodB was also crucial for survival under copper stress only in the Cu$^+$-efflux ATPase-deficient mutant copA$^-$

Similar to cadmium, copper is extruded from the bacterial cytoplasm mainly by the dedicated Cu$^+$-efflux ATPase CopA (Rensing *et al.*, 2000; Arguello *et al.*, 2007). In *R. gelatinosus* and *E. coli*, it was reported that accumulation of Cu$^+$ in *copA$^-$* mutant led to [4Fe-4S] degradation (Macomber and Imlay, 2009; Azzouzi *et al.*, 2013). To test whether Cu$^+$ could also lead to the induction of SodB in *copA$^-$* mutant, protein expression profiles and SOD *in-gel* activity of *R. gelatinosus* wild-type and *copA$^-$* cells grown in presence of excess CuSO$_4$ were compared to those of the ΔcadA strain grown in the presence of CdCl$_2$. In the wild-type background, cells

grown with excess CuSO$_4$ showed increased level of CopI, while amount and activity of SodB remained unchanged (Fig. 4A and B). In contrast, induction of CopI in the *copA*$^-$ cells was associated with an increased amount and activity of the superoxide dismutase SodB, with similar degree to Δ*cadA* cells exposed to CdCl$_2$ (Fig. 4A and B). Then, it is conceivable that SodB would also be required for tolerance to excess Cu$^+$. To address this, growth inhibition of the double mutant Δ*sodBcopA*$^-$ strain in presence of increasing concentration of CuSO$_4$ was monitored under photosynthetic and respiratory conditions and compared with Δ*sodB* or *copA*$^-$ single mutants (Fig. 4C and D). Disruption of the *sodB* gene in the wild-type background did not affect copper tolerance since Δ*sodB* mutant growth was comparable to that of the wild-type. However, disruption of *sodB* gene in the *copA*$^-$ mutant background led to a strong decrease in Cu$^+$ tolerance (Fig. 4C and D). Disc diffusion assay was also performed in presence of CuSO$_4$ and menadione, and the results indicated the hypersusceptibility of the Δ*sodBcopA*$^-$ strain to Cu^{2+} and superoxide on solid medium (Fig. S5). These results confirmed that SOD was also required for bacterial survival under copper stress when the Cu$^+$-efflux system was defective.

Altogether, association between the induction of SodB by metal excess and the hypersensitivity to the cognate metal in the SOD-efflux pump double mutant appeared to be common in *R. gelatinosus*. To understand whether this is a general phenomenon in bacteria, we tested induction of SOD by excess metal in different bacterial species.

Fe-Sod activity and amount were also increased in V. cholerae under Cd^{2+} stress

Vibrio cholerae is an aquatic bacterium but can infect human intestine to cause diarrhoeal diseases. *V. cholerae* encodes genes for two cytoplasmic SODs, the Mn-Sod (*vc2696* or *sodA*) and the Fe-Sod (*vc2045* or *sodB*) on the genome. However, *in-gel* SOD activity assay indicated that only SodB was active in our condition (Fig. 5A). *V. cholerae* also possesses Cd^{2+}/Zn^{2+}- and Cu$^+$-efflux ATPases, encoded by *zntA* (*vc1033*, hereafter referred to as *cadA* for clarity) and *copA* (*vc2215*) respectively. To assess the effect of increasing concentration of Cd^{2+} on SodB activity in *V. cholerae*, wild-type and the *cadA*$^-$ mutants were grown in the presence of excess CdCl$_2$ and the soluble fractions were analysed on non-denaturing PAGE for SOD activity. In the wild-type fractions, SodB activity was comparable between CdCl$_2$ exposed and non-exposed cells (Fig. 5B). In contrast, the *cadA*$^-$ mutant exposed to 5 μM CdCl$_2$ showed significant increase in SodB activity in comparison with non-exposed cells and the wild-type. Western blot analysis confirmed the increase in SodB amount only in the
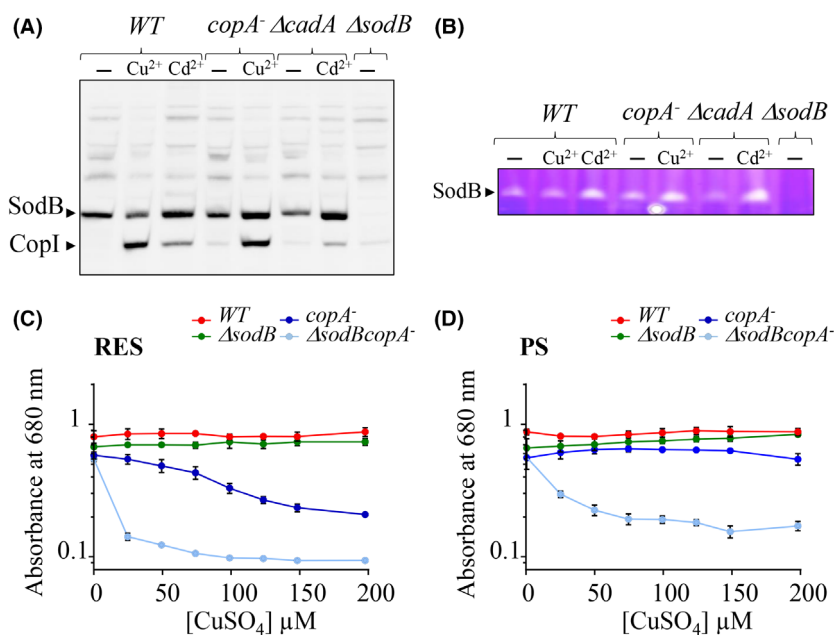

Fig. 4. Involvement of SodB in copper stress in *R. gelatinosus*. Western blot analysis of wild-type (*WT*), Δ*cadA*, *copA*$^-$ and Δ*sodB* mutants grown in malate medium supplemented or not (-) with 100 μM CdCl$_2$ (Cd^{2+}) or CuSO$_4$ (Cu^{2+}) (A). Cells were grown by photosynthesis, and total protein extracts from the same amount of cells (0.1 OD$_{680nm}$) were analysed by Western blot using the HRP-HisProbe. SOD activity assay on non-denaturing PAGE. Soluble fractions from the Δ*cadA*, *copA*, and Δ*sodB* mutants were separated on 15% PAGE (B). Dose–response curves of the *WT*, Δ*sodB*, *copA*$^-$ and Δ*sodBcopA*$^-$ strains. Cells were grown in presence of increasing concentration of CuSO$_4$ by respiration (C) or under photosynthesis condition (D) for 24 h. Results represent mean ± stdev from 3 independent experiments.
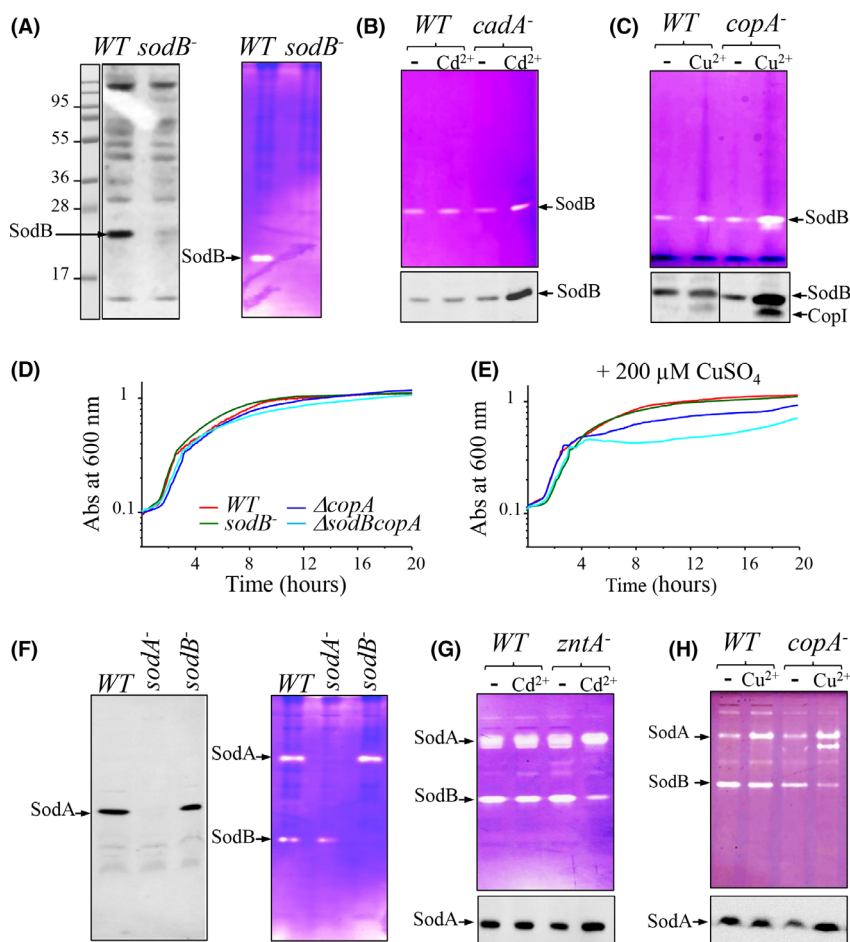
Fig. 5. SOD activity was induced in the ATPase mutants of *V. cholerae* and *E. coli*. Western blot and SOD *in-gel* activity assay of soluble fractions from wild-type (*WT*) and *SodB⁻* strains of *V. cholerae* (A). SodB activity and expression in *V. cholerae* were induced in the ATPase-deficient mutants *cadA⁻* and *copA⁻* in response to 5 μM CdCl₂ (Cd²⁺) (B) or 200 μM CuSO₄ (Cu²⁺) (C) as shown by the *in-gel* activity assay and on the Western blots. Effect of excess CuSO₄ on growth of the *V. cholerae* Δ*sodBcopA* deletion strain. *WT*, the single mutants Δ*copA, sodB⁻* and the Δ*sodBcopA* mutant were grown overnight in LB (D) or LB supplemented with 200 μM of CuSO₄ (E), growth was monitored at 600 nm with a Tecan Infinite. Western blot and SOD *in-gel* activity assay of soluble fractions from WT, *SodA⁻* and *SodB⁻* strains of *E. coli* (F). SodB activity was reduced, while SodA increased in the ATPase mutants *zntA⁻* and *copA⁻* in response to 20 μM CdCl₂ (Cd²⁺) (G) or 100 μM CuSO₄ (Cu²⁺) (H) as shown by the *in-gel* activity assays and on the Western blots.

cadA⁻-deficient mutant when exposed to CdCl₂ (Fig. 5B).

Similarly to the effect of cadmium in *cadA⁻*, both the activity and amount of SodB were also induced in the *copA⁻ V. cholerae* cells when challenged with 200 μM CuSO₄ (Fig. 5C). Note that induction of CopI (*vc0260*) was appreciated in *copA⁻* mutant and not in *cadA⁻ V. cholerae* cells (Fig. 5B and C). We then assessed the requirement of SodB for excess Cu⁺ tolerance in the absence of CopA. We introduced Δ*copA* mutation in *sodB⁻* strain and showed that the Δ*sodBcopA* double mutant has comparable growth rate in LB medium with the wild-type and the single mutants (Fig. 5D). When cells were challenged by 200 μM CuSO₄, *sodB* mutation did not affect copper tolerance, while Δ*copA* mutant showed slight growth defect (Fig. 5E). Importantly, the Δ*sodBcopA* double mutant

showed more sensitivity to copper than the Δ*copA* mutant (Fig. 5E). Altogether, even though the phenotype was not as strong as in *R. gelatinosus*, we concluded that SodB was also important for metal tolerance in *V. cholerae* given its high induction under excess metal and the sensitive phenotype of the double mutant.

Mn-Sod and Fe-Sod activity and amount, respectively, increased and decreased in response to excess Cd²⁺ or Cu⁺ in E. coli

In contrast to *R. gelatinosus* and *V. cholerae*, both the Fe-Sod (SodB) and the Mn-Sod (SodA) are active in *E. coli* (Carlioz and Touati, 1986) (Fig. 5F). Note that unlike *R. gelatinosus* and *V. cholerae*, *E. coli* SodB contains only four histidines in its amino terminus and is not detectable

on Western blot with the HisProbe. In contrast, SodA could be detected thanks to a five-histidine motif (Fig. 5F). Geslin *et al* reported that the absence of SodB and SodA in *E. coli* resulted in an increased sensitivity to Cd^{2+}, suggesting an interplay between SOD and excess cadmium (Geslin *et al.*, 2001). To address how *E. coli* handles the expression and activity of the two SODs in response to excess Cd^{2+} or Cu^+, impact of Cd^{2+} on SOD activity and amount in *E. coli,* wild-type and *cadA⁻* (*zntA⁻*) mutants were examined. *In-gel* SOD activity assay of soluble fractions showed no difference in SodB and SodA activities in the wild-type samples in response to 20 µM Cd^{2+} (Fig. 5G). On the contrary, in the *zntA⁻* mutant, exposure to 20 µM Cd^{2+} resulted in a decreased SodB activity concomitant to a slight increase in SodA activity. Western blot analyses did not show any significant increase in the amount of SodA in the wild-type samples, but showed a slight induction of SodA expression in the *zntA⁻* strain when exposed to excess $CdCl_2$.

Similar to the cadmium effect, the addition of 100 µM $CuSO_4$ to the growth medium of *copA⁻* strain significantly decreased the SodB and induced the SodA activity (Fig. 5H). This is in agreement with previous report in *E. coli* by Macomber and co-workers (Macomber *et al.*, 2007). Together, these findings clearly showed that both Cd^{2+} (redox non-active) and Cu^+ (redox-active) stress in *E. coli* resulted in a decreased Fe-Sod activity and increased Mn-Sod activity. This suggested that Cd^{2+} or Cu^+ may directly or indirectly activate SoxRS or trigger an iron limitation situation in *E. coli*.

Excess cadmium or copper led to the induction of SOD in P. aeruginosa, P. putida *and* B. subtilis

Previous transcriptional studies in *P. aeruginosa, P. putida* and in Gram + bacteria also reported slight increase of the SOD transcripts under many metal excess stresses, suggesting that SOD might protect cells under such conditions (Teitzel *et al.*, 2006; Cheng *et al.*, 2009; Yang *et al.*, 2012; Tarrant *et al.*, 2019).

P. aeruginosa genome encodes two different SODs, Mn-Sod (SodA) and Fe-Sod (SodB). SodB is the most abundant SOD in iron-replete condition and stationary growth phase, while SodA is only expressed under iron limitation (Martins *et al.*, 2018). We therefore examined whether excess Cd^{2+}(20 µM) or Cu^+ (200 µM) stress in the ATPase efflux mutants lacking CadA (ZntA) and CopA, respectively, affected activity and expression of SODs. Under both stresses, in the wild-type soluble fractions, SodB activity and expression were not affected by excess metal (Fig. 6A). In contrast, SodB activity and expression were increased in the *copA⁻* and *zntA⁻* mutants exposed to $CuSO_4$ and $CdCl_2$ respectively. These data showed that as in *R. gelatinosus* and *V. cholerae*, excess copper or cadmium induced the expression of SodB in *P. aeruginosa*.

In *P. putida,* in-gel SOD activity assay showed only one active band, which corresponded to a SodA-SodB heterodimer (Fig. 6B and (Heim *et al.*, 2003)). To check the effect of metal stress on this Sod heterodimer, wild-type and *copA* deletion mutants (Adaikkalam and Swarup, 2002) were subjected to 50 µM $CuSO_4$ copper stress and SOD activity and amount were assessed. For the wild-type, copper had no effect on SOD. In contrast, the *copA⁻* mutant showed increased SOD activity and amount under copper excess only (Fig. 6B). Both SodA and SodB are detectable by the HisProbe (both contain 5 histidine), and we were not able to discriminate between the two SODs due to a similar molecular weight. Nevertheless, excess copper was also linked to an increase in the superoxide dismutase activity in *P. putida*.
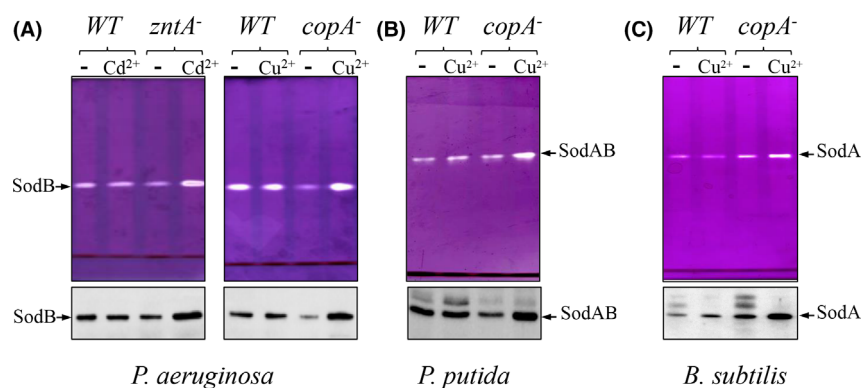
Fig. 6. SOD activity was induced in the ATPase-deficient mutants of *P. aeruginosa, P. putida* and *B. subtilis*. SodB activity and expression in *P. aeruginosa* were induced in the ATPase mutants *zntA⁻* and *copA⁻* in response to 20 µM $CdCl_2$ or 200 µM $CuSO_4$ as shown by the *in-gel* activity assay and on the Western blot (A). SOD (SodAB) activity and expression in *P. putida* were induced in the ATPase mutant *copA⁻* in response to 50 µM $CuSO_4$ (B). SodA activity and expression in *B. subtilis* were induced in the ATPase mutant *copA⁻* under 200 µM $CuSO_4$ stress (C).

Bacillus subtilis wild-type and $\Delta copA$ mutants were also grown in presence of $CuSO_4$, and their SOD activity and amount probed as above. Only one detectable band corresponding to the Mn-Sod was present in *B. subtilis* as previously reported (Henriques *et al.*, 1998; Inaoka *et al.*, 1998). The activity and amount of SodA were significantly induced in the $\Delta copA$ mutant challenged with 200 μM $CuSO_4$ in contrast to the wild-type (Fig. 6C).

Taken together, these data are in favour of a rather general mechanism involving the induction of SOD under the excess metal stress in bacteria. Importantly, the induction was triggered by both active and non-redox-active cations. The putative underlying molecular mechanisms that may govern such an induction are discussed below.

Discussion

Metal ions such as Fe^{2+}, Cu^+ or Co^{2+} are able to undergo different redox states and can induce in presence of oxygen, the production of reactive oxygen species *via* the Fenton and Haber–Weiss reactions (Elzanowska *et al.*, 1995; Gunther *et al.*, 1995). Even though Cd^{2+}, Zn^{2+} or Hg^{2+} are not redox active, they can also induce the production of ROS (Xu and Imlay, 2012; Norambuena *et al.*, 2019). Given their affinity for sulphur atoms, metal ions are also able to directly interact and inhibit the activity of many key enzymes whose assembly and/or activity depends on thiol/cysteine groups, even under strict anaerobic condition (Macomber and Imlay, 2009; Macomber and Hausinger, 2011; Barwinska-Sendra and Waldron, 2017). Therefore, accumulation of metal in the cell is a real threat that can ultimately lead to cell death if the detoxification systems fail to remove the excess. In this study, we showed that the cell protection, particularly against Cd^{2+} and Cu^+, relied primarily on the metal export system and then secondarily on the ROS detoxification enzymes. Indeed, the interplay between the two systems became manifest when both detoxification systems were inactivated. In *R. gelatinosus*, mutants devoid of both the efflux ATPase and the unique cytosolic SOD enzyme became much more sensitive to Cd^{2+} or Cu^+ than single mutants. This highlights (i) the critical role of the metal efflux ATPases in the protection of bacteria against metal homoeostasis dysregulation and (ii) the importance of superoxide detoxification system when metal homoeostasis was dysregulated. In our proposed toxicity model (Fig. 7), CadA or CopA protects the cell and prevents metal-related damage in the wild-type strain and SodB is constitutively expressed to a basal level. In the absence of CadA or CopA, accumulation of Cd^{2+} or Cu^+ in the cytoplasm would damage exposed [4Fe-4S] clusters and limit growth of the bacterium. Degradation of [4Fe-4S]
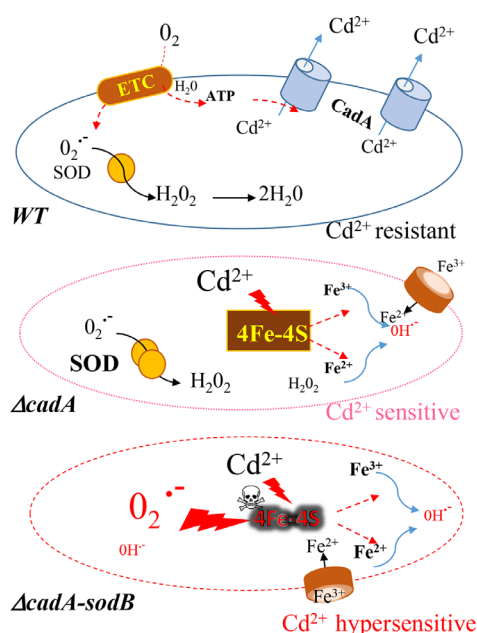

Fig. 7. Interplay between the metal efflux and ROS detoxifying system. Wild-type (WT) cells induce the expression of the ATPase CadA to prevent Cd^{2+} accumulation and related damages and SodB to scavenge superoxide. In the $\Delta cadA$ deficient mutant, accumulation of Cd^{2+} in the cytosol damage exposed [4Fe-4S] clusters, cells perceive the situation as an 'iron-starvation' condition and respond by increasing Fe^{2+} import presumably to rebuilt [4Fe-4S]. This led to the induction of the superoxide dismutase SodB in response to iron status. In cells defective in both metal and ROS detoxification systems, the concomitant accumulation of Cd^{2+} and ROS leads to metal hypersensitive cells and growth inhibition, because both superoxide and Cd^{2+} target enzymes with exposed [4Fe-4S] clusters. This imbalance and loss of [4Fe-4S] clusters is no longer tolerable by the bacterium.

clusters should increase temporarily the iron pool (released iron and/or iron uptake) that can ultimately generate oxidative stress if superoxide detoxification is not efficient. Like metals, reactive oxygen species such as superoxide damage [4Fe-4S] clusters and increase intracellular released iron (Keyer and Imlay, 1996; Imlay, 2019). Therefore, in cells defective for both metal and superoxide detoxification systems, the simultaneous accumulation of metal and superoxide was not endurable by the cell and inevitably led to metal hypersensitive cells and growth inhibition. Cells facing both excess Cd^{2+} and Cu^+ and superoxide accumulation would have significant decrease in their [4Fe-4S] clusters content. Moreover, Cu^+ and Cd^{2+} appeared to directly bind and inhibit components of the Fe-S biogenesis ISC machinery in bacteria (Chillappagari *et al.*, 2010; Tan *et al.*, 2017; Roy *et al.*, 2018), thus exacerbating the toxicity of metals and superoxide. Under such harsh conditions, stressed cells would not be able to repair or provide

sufficient active [Fe-S] clusters to sustain growth (Fig. 7). In addition, the presence of elevated level of superoxide with released iron from damaged clusters or imported by the uptake systems would participate in Fenton chemistry and catalyse hydroxyl radical formation in these cells, thereby contributing to cell growth inhibition. A similar scenario was reported to explain the toxicity of copper in macrophages, in which bacterial killing is caused by copper overloading and hydrogen peroxide production (White *et al.*, 2009). Our findings, with both redox-active Cu^+ and non-active Cd^{2+}, support this scenario and suggest that metal overloading and superoxide synergistically poison cells because they both destabilize exposed [4Fe-4S] clusters and likely target the same [4Fe-4S] enzymes.

One remarkable finding in this study is the induction of SOD expression and activity in the efflux ATPase mutants from different bacterial species when exposed to excess metal. This raised the question of the molecular mechanisms that underpinned SOD induction by excess Cd^{2+} or Cu^+. It is well established in *E. coli* and other bacteria that Mn-Sod and Fe-Sod expressions are partly regulated by the iron status within the cell. This regulation involves the Fur repressor and the sRNA RyhB that downregulate non-essential iron-containing proteins when iron is limiting (Masse and Gottesman, 2002; Imlay, 2019). Under such condition, the Fe-Sod expression is repressed, whereas the Mn-Sod is upregulated to convert superoxide into H_2O_2 and protect cells from oxidative stress. Excess Cu^{2+} or Cd^{2+} in bacteria and eukaryotes was shown to interfere with iron homoeostasis. Many studies suggest that excess Cd^{2+}, Ni^{2+}, Co^{2+}, Zn^{2+} or Cu^+ may generate an Fe-starvation signal and lead to the induction of iron uptake systems (Stadler and Schweyen, 2002; Yoshihara *et al.*, 2006; Houot *et al.*, 2007; Chillappagari *et al.*, 2010; Xu *et al.*, 2019). This could be a direct effect of [4Fe-4S] cluster degradation. Indeed, Keyer and Imlay elegantly showed that 'released iron' originating from [4Fe-4S] degradation was rapidly sequestrated, and iron uptake was then required to supply iron to the Fe-S machinery in response to peroxynitrite stress (Keyer and Imlay, 1997). In *E. coli*, we observed a decrease of the Fe-Sod and increase of the Mn-Sod, which suggest that under excess Cu^+ or Cd^{2+} stress, cells encounter a state of iron limitation. Furthermore, in *E. coli*, SoxR/SoxS directly induced the expression of the Mn-Sod in response to superoxide or redox-recycling compounds (Imlay, 2019). Therefore, if superoxide is produced under metal stress, then it could also explain the induction of Mn-Sod under Cu^+ or Cd^{2+} stress by SoxRS. Oxidation of the 2Fe-2S cluster of SoxR by superoxide or redox-active compounds activates SoxR (Imlay, 2013; Kobayashi, 2017; Imlay, 2019). Cu^+ is a potent

oxidant, Cd^{2+} is not. We observed the same SodA induction in cells challenged with excess Cu^+ or Cd^{2+}, suggesting that if Cu^+ and Cd^{2+} induction of SodA involves SoxRS, SoxR would be indirectly activated by these cations.

Unlike *E. coli*, *soxRS* genes are missing in *R. gelatinosus* genome. *V. cholerae* encodes SoxR homologue but not SoxS; however, the only available superoxide dismutase to protect the cell from the deleterious effects of superoxide is the iron-dependent SodB. Therefore, in these bacteria, there is no other choice but to express SodB in spite of the putative iron limitation status. To corroborate this hypothesis, we have shown that like iron starvation, Cu^+ and Cd^{2+} excess induced iron uptake system as attested by the accumulation of the iron-binding protein FbpA in the periplasm of *R. gelatinosus* (Steunou *et al.*, 2020b). The induction of Sod in the ATPase mutants is therefore indirect and is probably the consequence of iron homoeostasis dysregulation by excess Cd^{2+} or Cu^+.

Metals such as Cd^{2+} or Cu^+ can displace or replace Fe^{2+} in the ferric uptake regulator Fur and may therefore affect Fur-DNA binding (Adrait *et al.*, 1999; Mills & Marletta, 2005; Vitale *et al.*, 2009). Nevertheless, if Cd^{2+} or Cu^+ metallates Fur *in vivo* and allows binding to the Fur box, we may then expect a repression of the iron uptake systems and induction of the Fe-Sod. Our results showed, however, an induction of Fe-Sod and the FbpABC iron uptake system (Steunou *et al.*, 2020b), which rather suggest that Fur is unloaded in the presence of Cd^{2+} or Cu^+.

In *Vibrio tasmaniensis*, a pathogenic strain of oysters, the Mn-Sod is active. In this *vibrio*, it was shown that the Cu^+-efflux system (including CopA) and the ROS detoxification system (including SodA) were highly induced intracellularly (more than 50 fold) and that they are required for *vibrio* intracellular survival in phagocytes and cytotoxicity to haemocytes (Vanhove *et al.*, 2016). As for *V. cholerae*, for *Vibrio shiloi* (a coral pathogen), the Fe-Sod was required for survival of the bacterium in the coral ectodermal cells (Vanhove *et al.*, 2016).

In *P. aeruginosa*, transcriptional profiles of exposed cells to Cu^{2+} ions (Teitzel *et al.*, 2006), Cd^{2+} or Zn^{2+} nanoparticles also showed an increase in the relative amount of the Mn-Sod superoxide dismutase SodA transcript (Manara *et al.*, 2012; Yang *et al.*, 2012). The increase of SodA in these strains could be also related to iron homoeostasis, as several genes induced under iron-limiting condition were upregulated in copper-stressed cells. In *P. putida*, quantitative proteomic studies showed upregulation of SOD in Ni^{2+}, Co^{2+} or Cd^{2+}-treated cells, suggesting an increased production of superoxide radicals due to the presence of metal (Cheng *et al.*, 2009; Manara *et al.*, 2012; Ray *et al.*, 2013). These studies also pointed out for a role of iron

starvation in the induction of SOD since they also report the increased level of iron import proteins under metal stress. In Gram + bacteria, the superoxide dismutase SodM was also significantly induced by $CuSO_4$ in *Staphylococcus aureus* (Tarrant *et al.*, 2019). In *B. subtilis*, transcriptional profiles of exposed cells to Cu^{2+} ions also demonstrated that copper stress induced genes required for iron uptake and a slight increase in the SodA transcript (Chillappagari *et al.*, 2010). In the cyanobacterium *Synechocystis sp.* PCC 6803, high copper treatment also induced the expression of the iron superoxide dismutase *sodB* (Giner-Lamia *et al.*, 2014). Very recently, mercury (Hg^{2+}) was shown to induce ROS scavenging genes transcripts including the Mn-Sod in the thermophilic aerobe *Thermus thermophiles*. *T. thermophiles* Δsod mutant exhibited an increased sensitivity to Hg^{2+} (Norambuena *et al.*, 2019).

Collectively, these results showed that SOD was induced under metal excess stress in bacteria. The mechanisms of induction might be both direct and indirect and very likely involved iron homoeostasis dysregulation and SoxRS system when present as in *E. coli*. The data also showed that the SOD scavenging activity was vital when the metal efflux systems were defective. Increase in the SOD amount and activity would protect metal-exposed cells by decreasing superoxide concentration and hence would save some exposed [4Fe-4S] clusters from degradation (Imlay, 2019).

Extensive use of antibiotics in health care and agriculture has led to an increase in antibiotic resistance (Asante and Osei Sekyere, 2019). Copper and zinc exhibit antimicrobial properties and are used as alternatives to antibiotics in farming and agriculture. Nevertheless, the use of high concentrations of these cations led to environment contamination and to co-selection of antibiotic resistance genes (Baker-Austin *et al.*, 2006; Purves *et al.*, 2018; Rensing *et al.*, 2018; Bischofberger *et al.*, 2020). To avoid such impacts, we need to significantly reduce the concentration of metal in metal-based antimicrobial treatments. Our findings showed that superoxide detoxification system became determinant for bacterial survival under metal stress. Moreover, induction of SOD by excess metal appears to be a general phenomenon in bacteria; therefore, targeting the ROS defence system together with the metal efflux systems may allow lowering the concentration of metals in the metal-based antimicrobial treatments in agriculture and farming.

Experimental procedures

Bacterial strains and construction of mutants

Bacterial strains and plasmids used in this study are listed in Table S1. Standard methods were performed according to Sambrook *et al.* (1989) unless indicated otherwise. To inactivate *sodB*, a 1.7 kb fragment was amplified using the primers RG345_sodBF and RG346_sodBR (Table S2) and cloned into the PCR cloning vector pGEM-T to give *pGsodB*. *sodB* gene was inactivated by deletion of a 50 bp fragment and the insertion of the 1.2 kb Km cassette at the MscI and StuI sites within the *sodB* coding sequence. The resulting recombinant plasmid was designated *pGsodB::Km*. A 2.4 kb fragment obtained by PCR using RG369_xseAF and RG370_sodBR containing the entire *xseAsodB gene* was cloned into pGEM-T to give pG*xseAsodB*. *xseAsodB* was subcloned in pBBR1MCS-3 at the SmaI-SacI sites. The resulting plasmid was designated pB*xseAsodB*. From this plasmid, *xseA* was deleted by digestion with SacII and SmaI giving the pB*sodB* plasmid. Those plasmids were used for the complementation of Δ*sodB*. Transformation of *R. gelatinosus* cells was performed by electroporation (Ouchane *et al.*, 1996). The plasmid *pGsodB:: Km* was used to transform the wild-type, the *copA⁻* and Δ*cadA* strains. Transformants were selected on malate plates supplemented with the appropriate antibiotics under respiratory condition. Following transformant selection, template genomic DNA was prepared from the ampicillin-sensitive transformants and confirmation of the antibiotic resistance marker's presence at the desired locus was performed by PCR.

To construct Δ*copA* in *V. cholerae*, ∼ 600 bp fragments upstream and downstream to the *copA* were amplified using primers oYo848 and oYo849, and oYo850 and oYo851 respectively (Table S2). Resulting fragments were cloned into SmaI site of pCVD442 vector (Donnenberg and Kaper, 1991) using Gibson Assembly (Gibson *et al.*, 2009), resulting in pEYY345. Δ*copA* mutation was then introduced in C6706 (wild-type) and C6706 *sodB::Tn* strains, kindly provided by J. Mekalanos (Cameron *et al.*, 2008), by allelic exchange (Donnenberg and Kaper, 1991).

Single-gene deletion mutant library of *E. coli* (KEIO collection (Baba *et al.*, 2006)) was obtained from the National BioResource Project, National Institute of Genetics, Japan. *P. aeruginosa* mutants were obtained from the Comprehensive *P. aeruginosa* Transposon Mutant Library at the University of Washington Genome Center (Jacobs *et al.*, 2003). *P. putida* strains were kindly provided by Sanjay Swarup (Adaikkalam and Swarup, 2002), and *B. subtilis* strains were gift from Peter Graumann (Chillappagari *et al.*, 2010).

Cell preparation, growth and growth inhibition

Rubrivivax gelatinosus was grown at 30°C, in the dark aerobically (high oxygenation: 250 ml flasks containing 20 ml medium, referred to as respiratory condition) or under light microaerobically (in filled tubes with residual

oxygen in the medium, termed as photosynthetic condition) in malate growth medium. *E. coli, V. cholerae, B. subtilis* and *P. aeruginosa* were grown overnight at 37°C in LB medium. *P. putida* was grown at 30°C in LB medium. Antibiotics were added at following concentrations when appropriate: kanamycin, ampicillin, tetracycline, spectinomycin and trimethoprim (50 μg ml^{-1}), streptomycin (100 μg ml^{-1}).

Growth curves in respiratory condition were monitored at OD$_{680nm}$ with measurements taken every 15 min for 24 h using a Tecan Infinite M200 luminometer (Tecan, Mannerdorf, Switzerland). For growth inhibition under photosynthetic condition, strains were grown in filled tubes and OD$_{680nm}$ was measured after 24 h using the Tecan luminometer.

For disc diffusion assay, 200 μl (1 OD$_{680nm}$) of overnight grown cells was mixed with 7 ml semi-solid agar and uniformly spread onto solidified agar plates. Sterile discs (6 mm) were soaked with 10 μl of 10 mM menadione and placed in the middle of the plate. Plates were incubated overnight at 30°C under either photosynthetic or respiratory condition. The disc diffusion method was performed in triplicate, and the mean of the measured inhibition zones was calculated.

SOD in-gel activity assay on non-denaturing gel electrophoresis

About 20 μg of soluble proteins was separated on a 10% non-denaturing polyacrylamide gel and stained for SOD activity as described in Weydert and Cullen (2010), with minor modifications. Incubation with TEMED (0.85%) and Riboflavin-5-Phosphate (56 μM) was performed for 15 min at light and room temperature (RT), followed by the addition of nitroblue tetrazolium (2 mg ml^{-1}) and a 15 min incubation in the dark at RT. Gel was washed twice in ddH$_2$O and left in ddH$_2$O at RT on a light box until SOD-positive staining appeared.

Western blot and HisProbe-HRP detection

Equal amount of soluble proteins (20 μg) or disrupted cells (1 OD$_{680nm}$) when indicated was separated on SDS-PAGE and transferred onto a Hybond ECL Polyvinylidene difluoride membrane (GE Healthcare). Membrane was then probed with the HisProbe-HRP (horseradish peroxidase, from Pierce) according to the manufacturer's instruction. The HisProbe-HRP allows detection of proteins (including Sod) exhibiting at least five His residues in their N-ter domain. Those with only four His residues (*E. coli* SodB) are not detected with this probe. Positive bands were detected using a chemiluminescent HRP substrate according to the method of

Haan and Behrmann (Haan and Behrmann, 2007). Image capture was performed with a ChemiDoc camera system (Bio-Rad).

Conflict of interest

The authors declare that they have no conflicts of interest with the contents of this manuscript.

Author contributions

ASS and SO conceived of the study. ASS, MB, MLB, RT, AD, YY and SO acquired and analysed data. ASS, MB, AD, AKL and SO interpreted the data. ASS and SO wrote the manuscript.

References

Adaikkalam, V., and Swarup, S. (2002) Molecular characterization of an operon, cueAR, encoding a putative P1-type ATPase and a MerR-type regulatory protein involved in copper homeostasis in Pseudomonas putida. *Microbiology* **148:** 2857–2867.

Adrait, A., Jacquamet, L., Le Pape, L., Gonzalez de Peredo, A., Aberdam, D., Hazemann, J.L., *et al.* (1999) Spectroscopic and saturation magnetization properties of the manganese- and cobalt-substituted Fur (ferric uptake regulation) protein from *Escherichia coli*. *Biochemistry* **38:** 6248–6260.

Arguello, J.M., Eren, E., and Gonzalez-Guerrero, M. (2007) The structure and function of heavy metal transport P1B-ATPases. *Biometals* **20:** 233–248.

Asante, J., and Osei Sekyere, J. (2019) Understanding antimicrobial discovery and resistance from a metagenomic and metatranscriptomic perspective: advances and applications. *Environ Microbiol Rep* **11:** 62–86.

Azzouzi, A., Steunou, A.S., Durand, A., Khalfaoui-Hassani, B., Bourbon, M.L., Astier, C., *et al.* (2013) Coproporphyrin III excretion identifies the anaerobic coproporphyrinogen III oxidase HemN as a copper target in the Cu$^+$-ATPase mutant *copA$^-$* of *Rubrivivax gelatinosus*. *Mol Microbiol* **88:** 339–351.

Baba, T., Ara, T., Hasegawa, M., Takai, Y., Okumura, Y., Baba, M., *et al.* (2006) Mori H (2006) construction of *Escherichia coli* K-12 in-frame, single-gene knockout mutants: the Keio collection. *Mol Syst Biol* **2:** 0008.

Baker-Austin, C., Wright, M.S., Stepanauskas, R., and McArthur, J.V. (2006) Co-selection of antibiotic and metal resistance. *Trends Microbiol* **14:** 176–182.

Ballabio, C., Panagos, P., Lugato, E., Huang, J.H., Orgiazzi, A., Jones, A., *et al.* (2018) Copper distribution in European topsoils: an assessment based on LUCAS soil survey. *Sci Total Environ* **636:** 282–298.

Barwinska-Sendra, A., and Waldron, K.J. (2017) The role of intermetal competition and mis-metalation in metal toxicity. *Adv Microb Physiol* **70:** 315–379.

Beyer, W., Imlay, J., and Fridovich, I. (1991) Superoxide dismutases. *Prog Nucleic Acid Res Mol Biol* **40:** 221–253.

Bischofberger, A.M., Baumgartner, M., Pfrunder-Cardozo, K.R., Allen, R.C., and Hall, A.R. (2020) Associations between sensitivity to antibiotics, disinfectants and heavy metals in natural, clinical and laboratory isolates of *Escherichia coli*. *Environ Microbiol*. https://doi.org/10.1111/1462-2920.14986

Cameron, D.E., Urbach, J.M., and Mekalanos, J.J. (2008) A defined transposon mutant library and its use in identifying motility genes in *Vibrio cholerae*. *Proc Natl Acad Sci USA* **105:** 8736–8741.

Capdevila, D.A., Edmonds, K.A., and Giedroc, D.P. (2017) Metallochaperones and metalloregulation in bacteria. *Essays Biochem* **61:** 177–200.

Carlioz, A., and Touati, D. (1986) Isolation of superoxide dismutase mutants in *Escherichia coli*: is superoxide dismutase necessary for aerobic life? *The EMBO journal* **5:** 623–630.

Chandrangsu, P., Rensing, C., and Helmann, J.D. (2017) Metal homeostasis and resistance in bacteria. *Nat Rev Microbiol* **15:** 338–350.

Cheng, Z., Wei, Y.Y., Sung, W.W., Glick, B.R., and McConkey, B.J. (2009) Proteomic analysis of the response of the plant growth-promoting bacterium *Pseudomonas putida* UW4 to nickel stress. *Proteome Sci* **7:** 18.

Chillappagari, S., Seubert, A., Trip, H., Kuipers, O.P., Marahiel, M.A., and Miethke, M. (2010) Copper stress affects iron homeostasis by destabilizing iron-sulfur cluster formation in *Bacillus subtilis*. *J Bacteriol* **192:** 2512–2524.

Dietrich, L.E., Teal, T.K., Price-Whelan, A., and Newman, D.K. (2008) Redox-active antibiotics control gene expression and community behavior in divergent bacteria. *Science* **321:** 1203–1206.

Djoko, K.Y., and McEwan, A.G. (2013) Antimicrobial action of copper is amplified via inhibition of heme biosynthesis. *ACS Chem Biol* **8:** 2217–2223.

Donnenberg, M.S., and Kaper, J.B. (1991) Construction of an eae deletion mutant of enteropathogenic *Escherichia coli* by using a positive-selection suicide vector. *Infect Immun* **59:** 4310–4317.

Elzanowska, H., Wolcott, R.G., Hannum, D.M., and Hurst, J.K. (1995) Bactericidal properties of hydrogen peroxide and copper or iron-containing complex ions in relation to leukocyte function. *Free Radic Biol Med* **18:** 437–449.

Geslin, C., Llanos, J., Prieur, D., and Jeanthon, C. (2001) The manganese and iron superoxide dismutases protect *Escherichia coli* from heavy metal toxicity. *Res Microbiol* **152:** 901–905.

Gibson, D.G., Young, L., Chuang, R.Y., Venter, J.C., Hutchison, C.A. 3rd, and Smith, H.O. (2009) Enzymatic assembly of DNA molecules up to several hundred kilobases. *Nat Methods* **6:** 343–345.

Giner-Lamia, J., Lopez-Maury, L., and Florencio, F.J. (2014) Global transcriptional profiles of the copper responses in the cyanobacterium *Synechocystis* sp. PCC 6803. *PLoS ONE* **9:** e108912.

Gunther, M.R., Hanna, P.M., Mason, R.P., and Cohen, M.S. (1995) Hydroxyl radical formation from cuprous ion and hydrogen peroxide: a spin-trapping study. *Arch Biochem Biophys* **316:** 515–522.

Haan, C., and Behrmann, I. (2007) A cost effective non-commercial ECL-solution for Western blot detections yielding strong signals and low background. *J Immunol Methods* **318:** 11–19.

Heim, S., Ferrer, M., Heuer, H., Regenhardt, D., Nimtz, M., and Timmis, K.N. (2003) Proteome reference map of Pseudomonas putida strain KT2440 for genome expression profiling: distinct responses of KT2440 and Pseudomonas aeruginosa strain PAO1 to iron deprivation and a new form of superoxide dismutase. *Environ Microbiol* **5:** 1257–1269.

Helbig, K., Grosse, C., and Nies, D.H. (2008) Cadmium toxicity in glutathione mutants of *Escherichia coli*. *J Bacteriol* **190:** 5439–5454.

Henriques, A.O., Melsen, L.R., and Moran, C.P. Jr (1998) Involvement of superoxide dismutase in spore coat assembly in *Bacillus subtilis*. *J Bacteriol* **180:** 2285–2291.

Houot, L., Floutier, M., Marteyn, B., Michaut, M., Picciocchi, A., Legrain, P., *et al.* (2007) Cadmium triggers an integrated reprogramming of the metabolism of Synechocystis PCC6803, under the control of the Slr1738 regulator. *BMC Genom* **8:** 350.

Imlay, J.A. (2003) Pathways of oxidative damage. *Annu Rev Microbiol* **57:** 395–418.

Imlay, J.A. (2013) The molecular mechanisms and physiological consequences of oxidative stress: lessons from a model bacterium. *Nat Rev Microbiol* **11:** 443–454.

Imlay, J.A. (2019) Where in the world do bacteria experience oxidative stress? *Environ Microbiol* **21:** 521–530.

Inaoka, T., Matsumura, Y., and Tsuchido, T. (1998) Molecular cloning and nucleotide sequence of the superoxide dismutase gene and characterization of its product from *Bacillus subtilis*. *J Bacteriol* **180:** 3697–3703.

Jacobs, M.A., Alwood, A., Thaipisuttikul, I., Spencer, D., Haugen, E., Ernst, S., *et al.* (2003) Comprehensive transposon mutant library of *Pseudomonas aeruginosa*. *Proc Natl Acad Sci USA* **100:** 14339–14344.

Keyer, K., and Imlay, J.A. (1996) Superoxide accelerates DNA damage by elevating free-iron levels. *Proc Natl Acad Sci USA* **93:** 13635–13640.

Keyer, K., and Imlay, J.A. (1997) Inactivation of dehydratase [4Fe-4S] clusters and disruption of iron homeostasis upon cell exposure to peroxynitrite. *J Biol Chem* **272:** 27652–27659.

Kobayashi, K. (2017) Sensing mechanisms in the Redox-Regulated, [2Fe-2S] cluster-containing, bacterial transcriptional factor SoxR. *Acc Chem Res* **50:** 1672–1678.

Krumschnabel, G., Manzl, C., Berger, C., and Hofer, B. (2005) Oxidative stress, mitochondrial permeability transition, and cell death in Cu-exposed trout hepatocytes. *Toxicol Appl Pharmacol* **209:** 62–73.

Macomber, L., and Hausinger, R.P. (2011) Mechanisms of nickel toxicity in microorganisms. *Metallomics* **3**: 1153–1162.

Macomber, L., and Imlay, J.A. (2009) The iron-sulfur clusters of dehydratases are primary intracellular targets of copper toxicity. *Proc Natl Acad Sci USA* **106**: 8344–8349.

Macomber, L., Rensing, C., and Imlay, J.A. (2007) Intracellular copper does not catalyze the formation of oxidative DNA damage in *Escherichia coli. J Bacteriol* **189**: 1616–1626.

Manara, A., DalCorso, G., Baliardini, C., Farinati, S., Cecconi, D., and Furini, A. (2012) *Pseudomonas putida* response to cadmium: changes in membrane and cytosolic proteomes. *J Proteome Res* **11**: 4169–4179.

Martins, D., McKay, G., Sampathkumar, G., Khakimova, M., English, A.M., and Nguyen, D. (2018) Superoxide dismutase activity confers (p)ppGpp-mediated antibiotic tolerance to stationary-phase *Pseudomonas aeruginosa. Proc Natl Acad Sci USA* **115**: 9797–9802.

Masse, E., and Gottesman, S. (2002) A small RNA regulates the expression of genes involved in iron metabolism in Escherichia coli. *Proc Natl Acad Sci USA* **99**: 4620–4625.

Mills, S.A., and Marletta, M.A. (2005) Metal binding characteristics and role of iron oxidation in the ferric uptake regulator from *Escherichia coli. Biochemistry* **44**: 13553–13559.

Norambuena, J., Hanson, T.E., Barkay, T., and Boyd, J.M. (2019) Superoxide dismutase and Pseudocatalase increase tolerance to Hg(II) in Thermus thermophilus HB27 by maintaining the reduced Bacillithiol Pool. *MBio* **10**: 1–14.

Nunes, I., Jacquiod, S., Brejnrod, A., Holm, P.E., Johansen, A., Brandt, K.K., *et al.* (2016) Coping with copper: legacy effect of copper on potential activity of soil bacteria following a century of exposure. *FEMS Microbiol Ecol* **92**: fiw175.

Ouchane, S., Picaud, M., Reiss-Husson, F., Vernotte, C., and Astier, C. (1996) Development of gene transfer methods for *Rubrivivax gelatinosus* S1: construction, characterization and complementation of a puf operon deletion strain. *Mol Gen Genet* **252**: 379–385.

Purves, J., Thomas, J., Riboldi, G.P., Zapotoczna, M., Tarrant, E., Andrew, P.W., *et al.* (2018) A horizontally gene transferred copper resistance locus confers hyperresistance to antibacterial copper toxicity and enables survival of community acquired methicillin resistant *Staphylococcus aureus* USA300 in macrophages. *Environ Microbiol* **20**: 1576–1589.

Ray, P., Girard, V., Gault, M., Job, C., Bonneu, M., Mandrand-Berthelot, M.A., *et al.* (2013) *Pseudomonas putida* KT2440 response to nickel or cobalt induced stress by quantitative proteomics. *Metallomics* **5**: 68–79.

Rensing, C., Fan, B., Sharma, R., Mitra, B., and Rosen, B.P. (2000) CopA: An *Escherichia coli* Cu(I)-translocating P-type ATPase. *Proc Natl Acad Sci USA* **97**: 652–656.

Rensing, C., Moodley, A., Cavaco, L.M., and McDevitt, S.F. (2018) Resistance to metals used in agricultural production. *Microbiol Spectr* **6**: 1–24.

Roy, P., Bauman, M.A., Almutairi, H.H., Jayawardhana, W.G., Johnson, N.M., and Torelli, A.T. (2018) Comparison of the response of bacterial IscU and SufU to Zn(2+) and select transition-metal ions. *ACS Chem Biol* **13**: 591–599.

von Rozycki, T., and Nies, D.H. (2009) Cupriavidus metallidurans: evolution of a metal-resistant bacterium. *Antonie Van Leeuwenhoek* **96**: 115–139.

Sambrook, J., Fritsch, E.F., and Maniatis, T. (1989) *Molecular Cloning, A Laboratory Manual*, 2nd edn. New York, NY: Cold Spring Harbor.

Stadler, J.A., and Schweyen, R.J. (2002) The yeast iron regulon is induced upon cobalt stress and crucial for cobalt tolerance. *J Biol Chem* **277**: 39649–39654.

Steunou, A.S., Durand, A., Bourbon, M.L., Babot, M., Liotenberg, S., and Ouchane, S. (2020a) Cadmium and Copper Cross-tolerance. Cu+ alleviates Cd2+ toxicity, and both cations target the porphyrin biosynthesis pathway in *Rubrivivax gelatinosus. Front Microbiol* (in press) https://doi.org/10.3389/fmicb.2020.00893

Steunou, A.S., Bourbon, M.L., Babot, M., Durand, A., Liotenberg, S., Yamaichi, Y., and Ouchane, S. (2020b) Increasing the copper sensitivity of microorganisms by restricting iron supply, a strategy for bio-management practices. *Microb Biotechnol* (in press), https://doi.org/10.1111/1751-7915.13590

Tan, G., Yang, J., Li, T., Zhao, J., Sun, S., Li, X., *et al.* (2017) Anaerobic Copper Toxicity and Iron-Sulfur Cluster Biogenesis in *Escherichia coli. Appl Environ Microbiol* **83**: 17.

Tarrant, E., Riboldi, P.G., McIlvin, M.R., Stevenson, J., Barwinska-Sendra, A., Stewart, L.J., *et al.* (2019) Copper stress in *Staphylococcus aureus* leads to adaptive changes in central carbon metabolism. *Metallomics* **11**: 183–200.

Teitzel, G.M., Geddie, A., De Long, S.K., Kirisits, M.J., Whiteley, M., and Parsek, M.R. (2006) Survival and growth in the presence of elevated copper: transcriptional profiling of copper-stressed Pseudomonas aeruginosa. *J Bacteriol* **188**: 7242–7256.

Turner, R.J. (2017) Metal-based antimicrobial strategies. *Microbial Biotechnol* **10**: 1062–1065.

Vanhove, A.S., Rubio, T.P., Nguyen, A.N., Lemire, A., Roche, D., Nicod, J., *et al.* (2016) Copper homeostasis at the host vibrio interface: lessons from intracellular vibrio transcriptomics. *Environ Microbiol* **18**: 875–888.

Vitale, S., Fauquant, C., Lascoux, D., Schauer, K., Saint-Pierre, C., and Michaud-Soret, I. (2009) A ZnS(4) structural zinc site in the *Helicobacter pylori* ferric uptake regulator. *Biochemistry* **48**: 5582–5591.

Weydert, C.J., and Cullen, J.J. (2010) Measurement of superoxide dismutase, catalase and glutathione peroxidase in cultured cells and tissue. *Nat Protoc* **5**: 51–66.

White, C., Lee, J., Kambe, T., Fritsche, K., and Petris, M.J. (2009) A role for the ATP7A copper-transporting ATPase in macrophage bactericidal activity. *J Biol Chem* **284**: 33949–33956.

Xu, F.F., and Imlay, J.A. (2012) Silver(I), mercury(II), cadmium(II), and zinc(II) target exposed enzymic iron-sulfur clusters when they toxify *Escherichia coli. Appl Environ Microbiol* **78**: 3614–3621.

Xu, Z., Wang, P., Wang, H., Yu, Z.H., Au-Yeung, H.Y., Hirayama, T., *et al.* (2019) Zinc excess increases cellular demand for iron and decreases tolerance to copper in *Escherichia coli. J Biol Chem* **294**: 16978–16991.

Yang, Y., Mathieu, J.M., Chattopadhyay, S., Miller, J.T., Wu, T., Shibata, T., *et al.* (2012) Defense mechanisms of Pseudomonas aeruginosa PAO1 against quantum dots and their released heavy metals. *ACS Nano* **6:** 6091–6098.

Yoshihara, T., Hodoshima, H., Miyano, Y., Shoji, K., Shimada, H., and Goto, F. (2006) Cadmium inducible Fe deficiency responses observed from macro and molecular views in tobacco plants. *Plant Cell Rep* **25:** 365–373.

Supporting information

Additional supporting information may be found online in the Supporting Information section at the end of the article.

Table S1. Bacterial strains and plasmids used in this work.

Table S2. DNA primers used in this work.

Fig. S1. A 22 kDa protein was induced in the Cd^{2+}-ATPase deficient mutants under respiration. Induction of SodB in *R. gelatinosus* wild-type (*WT*), *cadR$^-$* and $\Delta cadA$ strains with the increase of $CdCl_2$ concentration. Cells were grown under respiration. Total protein extracts from the same amount of cells ($OD_{680nm} = 1$) were separated on 15% SDS-PAGE and analyzed by western blot using the HisProbe.

Fig. S2. XseA is not required for menadione tolerance. A. Menadione disc-diffusion assay (as described in Experimental procedures) results showing the complementation by pB*xseAsodB* and pB*sodB*. pBTc: empty plasmid. B. *sodB* constructs used in this work. pG*sodB*::Km was used to generate the $\Delta sodB$ mutant. pB derivatives (pB*xseAsodB* and pB*sodB*) were used for complementations of $\Delta sodB$ strain.

Fig. S3. Genetic organization of *xseA* s*odB* orfs. A. *xseA-sodB* gene fusion. *xseA* coding sequence is in blue and *sodB* in red. No stop codon was found between the two orfs. Putative promoters and transcripts and primers used in RT-PCR are indicated. B. Protein sequence of the fusion. The five His detected by the HisProbe in SodB are shown in black and boldstyle. C. Analysis of *sodB* expression by RT-PCR. Total RNA from wild-type (*WT*) and $\Delta sodB$ strains grown under respiration was extracted according to Steunou *et al.* (2004). 2 μg of total RNA was reverse transcribed with the superscript II (Invitrogen) using the specific *sodB* primer RG348. 2 μl of the RT reaction was used for the PCR. We used either the primers RG433-RG434 specific to *xseA* or the RG347–RG348 primers specific to *sodB*. Both PCRs were positive showing the presence of the *xseAsodB* transcript (arrow). Genomic DNA and 16SrRNA were used for controls. This experiment suggested the presence of *xseA-sodB* transcript but does not exclude the presence of an internal promoter upstream of *sodB*. Putative promoters are shown in gray.

Fig. S4. Effect of Cd^{2+} and menadione stress in $\Delta sodB$, and $\Delta cadAsodB$ strains. A. Menadione disc-diffusion assay. Plates were incubated at 30°C overnight either under photosynthetic (PS) or respiratory (RES) conditions. B. Western blot analysis of wild-type (*WT*), $\Delta sodB$, $\Delta cadA$, and $\Delta cadA$-*sodB* strains grown by photosynthesis with (50 μM) or without (−) cadmium, showing the induction of SodB. C. Effect of Cd^{2+} and menadione stress in $\Delta sodB$, and $\Delta cadAsodB$ strains. Menadionedisc-diffusion assay in plates supplemented or not with 25 mM $CdCl_2$. Plates were incubated at 30°C over night under aerobic respiration conditions. The simultaneous presence of Cd^{2+} and menadione is deleterious for the $\Delta cadAsodB$ hyper-sensitive strain.

Fig. S5. Effect of $CuSO_4$ and menadione stress in the wild-type (*WT*), $\Delta sodB$, *copA$^-$*, and $\Delta sodBcopA^-$ strains. Menadione disc-diffusion assay in plates supplemented or not with 25 mM $CuSO_4$ (as described in Experimental procedures). Plates were incubated at 30°C overnight under aerobic respiration conditions. The simultaneous presence of Cu^{2+} and menadione is deleterious for the $\Delta sodBcopA^-$ hyper-sensitive strain.